Gasification performance of Spirulina microalgae_A thermodynamic study with tar formation

by Arif Hidayat

Submission date: 05-Apr-2023 08:12PM (UTC+0700)
Submission ID: 2056569198
File name: pirulina_microalgae_A_thermodynamic_study_with_tar_formation.pdf (2.62M)
Word count: 8395
Character count: 41923

Fuel 241 (2019) 372–381

Contents lists available at ScienceDirect

Fuel

journal homepage: www.elsevier.com/locate/fuel

Full Length Article

Gasification performance of *Spirulina* microalgae – A thermodynamic study with tar formation

Muflih A. Adnan[a,c,1], Qingang Xiong[b,1], Arif Hidayat[a], Mohammad M. Hossain[c,d,*]

[a] Department of Chemical Engineering, Islamic University of Indonesia, Sleman, Daerah Istimewa Yogyakarta 55584, Indonesia
[b] IT Innovation Center, General Motors, Warren, MI 48092, USA
[c] Department of Chemical Engineering, King Fahd University of Petroleum & Minerals, Dhahran 31261, Saudi Arabia
[d] Center of Research Excellence in Nanotechnology, King Fahd University of Petroleum & Minerals, Dhahran 31261, Saudi Arabia

ARTICLE INFO

Keywords:
Biomass gasification
Spirulina microalgae
Tar formation
Thermodynamic analysis
Optimization

ABSTRACT

In this work, the performance of a novel configuration for *Spirulina* microalgae gasification was investigated through an improved thermodynamic model using Aspen Plus. Compared with existing thermodynamic models, tar formation is included in the improved counterpart. The proposed novel gasification process consists of four primary zones: (i) pyrolysis, (ii) combustion, (iii) gasification, and (iv) optimization. First, the modeling results were compared against experimental values, where a good agreement (relative error < 10%) was obtained under identical operating conditions. Then, performance of the novel gasification configuration was studied using the developed improved thermodynamic model at various operating conditions. Metrics such as gasification system efficiency, syngas composition and cold gas efficiency were used to measure the performance. It was found that incorporation of the optimization zone improves the concentration of CO and H_2 at the controlled use of gasifying agents. Moreover, injection of suitable amount of gasifying agents enhances the gasification performance. Finally, the effects of O_2 equivalence ratio and steam injection on the system performance were investigated.

1. Introduction

In recent years, besides traditional agricultural biomass, a special type of biomass, microalgae, has received considerable attention as a clean energy source to substitute fossil fuels due to the increased concern on energy security as well as environmental sustainability [1]. Biomass from different sources including terrestrial biomass and marine biomass is considered as a potential candidate to substitute the fossil fuels given its advantages over fossil fuels in term of environment issue (e.g., carbon neutral cycle). Recently, on purpose marine biomass such as microalgae has received a growing attention as a clean energy source attributable to its advantages over terrestrial biomass including its ability to recover CO_2 through photosynthesis way during their growing period, tolerance with nutrients in the water, higher photosynthesis efficiency and shorter growth cycle [2]. The use of microalgae emits notably low SO_x emission due to its minimum concentration of sulfur. In addition, even microalgae consists of high-protein, indicating considerable amount of nitrogen element, the NO_x formation during gasification process could be minimized by selecting proper gasifying agent (i.e., O_2, CO_2) [3,4]. Indeed, production cost of microalgae is a major consideration for commercialization of microalgae for biofuels. The selection of proper nutrients, water and CO_2 could potentially cut the production cost by > 50% [5]. Furthermore, the production cost can be reduced by taking suitable land for cultivation of microalgae [6] and the harvesting method [7]. Among various approaches to convert microalgae into biofuels, gasification through which a mixture of incondensable gas such as H_2, CO, CH_4 and CO_2 is produced, has been widely viewed as a promising way due to its relatively high energy conversion efficiency [2].

However, at industrial scale, effective gasification of microalgae is still limited largely due to the existence of tar, a complex mixture of aromatic hydrocarbons [8]. Because of the existence of tar which comes out along with the produced incondensable gas, gasification efficiency can be significantly diminished [9]. Therefore, tar concentration during the gasification of microalgae should be kept as minimum as possible. In most instances, tar concentration can be reduced using separation either by dry treatment (i.e., cyclone, filters, etc.) or wet treatment (i.e., spray towers, wet cyclones, etc.). Although separation has been

* Corresponding author at: Department of Chemical Engineering, King Fahd University of Petroleum & Minerals, Dhahran 31261, Saudi Arabia.
E-mail address: mhossain@kfupm.edu.sa (M.M. Hossain).
[1] These authors contributed equally to this work.

https://doi.org/10.1016/j.fuel.2018.12.061
Received 1 September 2018; Received in revised form 10 December 2018; Accepted 11 December 2018
Available online 18 December 2018
0016-2361/

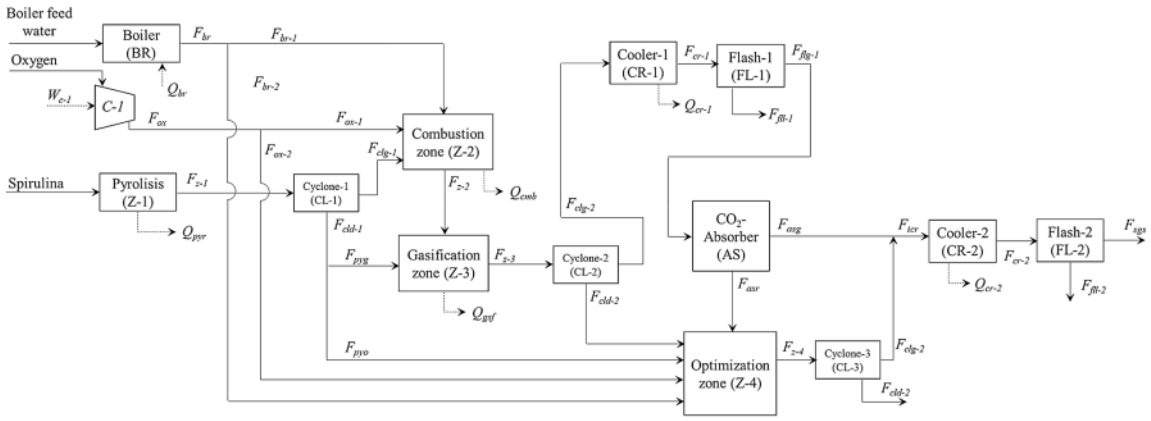

Fig. 1. Schematic diagram of the proposed gasification process for *Spirulina*.

demonstrated as an effective way to remove tar from the produced incondensable gas, it is not able to fully preserve the high gasification efficiency given tar is wasted instead of being converted to incondensable gas [10]. Moreover, post-processing the separated tar requires additional energy, which will further decrease the overall gasification efficiency [1,11]. Thus, it is more feasible to directly convert tar into incondensable combustible gas.

During microalgae gasification, tar is primarily formed in the pyrolysis step which occurs at relatively low temperature. In principle, direct conversion of tar into incondensable combustible gas can be achieved through three approaches, i.e., (i) increasing the gasification temperature, (ii) employment of tar cracking catalysts, and (iii) novel gasifier design. However, thermal cracking of tar at high temperature is costly as this is an energy intensive process [1,12]. In general, using catalysts should be a proper way to increase tar conversion at relatively low temperature [1,13]. However, it is highly possible for catalysts to suffer from the problems of deactivation due to pore blockage by coke and degradation of mechanical strengths [14–16]. For design of novel gasifiers, in recent years many investigations have shown that it is an efficient way to increase tar conversion and gasification efficiency. For example, Susanto and Beenackers [17] proposed a new design on a continuous downdraft gasifier for woody biomass, in which an internal cycle is introduced. With such novel design, tar produced from the pyrolysis zone is cracked in the combustion zone, through which the final collected tar concentration decreases by 97% (from 1410 mg·Nm^{-3} to 48 mg·Nm^{-3}). Similarly, Brandt et al. [18] successfully reduced tar content below 15 mg·Nm^{-3} using the design of two-stage gasifier with a dry wood as the feedstock. Therefore, it could be anticipated that novel design of gasifier could significantly increase the efficiency of microalgae gasification.

In our previous work [19], a gasification system including a CO_2-absorber to upgrade the syngas quality by removing CO_2 from the syngas stream was proposed and assessed. It was proved to be very efficient for microalgae gasification. In this study, such novel gasification design is further enhanced by realizing the in-situ utilization of pure CO_2 as the side product through facilitating the Bouduard reaction to enhance the char and CO_2 conversion into CO, which is usually used in a direct carbon solid oxide fuel cell (SOFC) [20]. The improved configuration consists of pyrolysis, combustion, gasification, and optimization stages, respectively, with a number of advantages such as production of clean syngas due to an effective tar conversion and in-situ utilization of CO_2.

Assessing the performance of a novel design for microalgae gasification is critical to its subsequent optimization and scale-up processes. However, it is rather difficult, even if possible, to use the traditional experimental approach to conduct such laborious, high-cost and time-consuming work, especially for a large-scale microalgae gasification [21]. Thermodynamic modeling, where steady-state equilibrium physicochemical principles are applied to predict the overall reactor outcome, has been widely viewed as a promising way to quickly estimate the overall performance of biomass gasification with reasonable accuracy [22–25]. For this reason, thermodynamic modeling has also been largely employed to simulate biomass gasification and evaluate the performance of novel gasifier designs [26,27]. This is also the case to microalgae gasification [22,23]. However, most thermodynamic modeling of microalgae gasification uses relatively simplified reactions to model the tar formation and conversion. This will definitely lower the overall prediction accuracy for thermodynamic modeling of microalgae gasification. Due to the high nitrogenated content in microalgae, many studies have revealed that it is reasonable to approximate tar as nitrogenated aromatic hydrocarbon to preserve engineering accuracy [28,29]. Therefore, such tar approximation is adopted in our current thermodynamic modeling of microalgae gasification [30].

In this work, a comprehensive thermodynamic modeling of the foregoing mentioned new configuration for microalgae gasification was conducted using Aspen Plus. The single-species microalgae, *Spirulina*, was selected as the feedstock and tar was modeled as a mixture of nitrogenated aromatic hydrocarbons. *Spirulina* contains high concentration of protein, which is favorable for production of oil during pyrolysis stage [31]. Furthermore, the vaporized oil is converted into syngas as the major gasification product. First, the thermodynamic modeling was validated against experimental results to prove its accuracy. Then, performance of the new *Spirulina* gasification system was analyzed with respect to gasification system efficiency, syngas composition and cold gas efficiency. Finally, the flow rates of oxygen and steam were varied to investigate their effects on gasification performance for optimal operation of the new design.

2. Description of the novel design

The proposed novel design of microalgae gasification process is shown in Fig. 1, where four major zones are involved, i.e., pyrolysis zone, combustion zone, gasification zone, and optimization zone. The gasifying agents are steam and high-purity oxygen. The ultimate and proximate analysis of the feedstock *Spirulina* including its heating value are summarized in Table 1. The *Spirulina* feedstock including its properties (i.e., ultimate, proximate and high heating value) for simulation is adapted from the one used by Hong et al. [31]. The actual operation of *Spirulina* gasification in this novel configuration can be majorly described as follows. At the inlet, *Spirulina* is continuously fed at constant flow rate of 100 kg/h. The feedstock first enters the pyrolysis zone (Z-1). In Z-1, moisture content in *Spirulina* evaporates first due to high

Table 1
Properties of *Spirulina* [31].

Proximate, % mass	
Moisture	6.7
Volatile matters	73.5
Fixed carbon	13.2
Ash	6.6
Ultimate, % mass	
C	49.8
H	6.6
O	31.9
N	11.0
S	0.7
HHV, MJ/kg	15.1

temperature. Then, *Spirulina* is decomposed into solid (i.e., char) and gaseous products including water vapor, permanent gases (CO, H_2, CH_4 and CO_2) and tars. These pyrolysis products are sent to the cyclone 1 (CL-1) to separate the solid products from the gaseous products. The solid products are further split into two streams: one to the gasification zone (Z-3) and the other to the optimization zone (Z-4). At the same time, the gaseous products are directed to the combustion zone (Z-2). In Z-2, the gaseous products contact with the gasifying agents and the tar concentration decays due to its conversion to permanent gases. After that, the products from Z-2 are sent to Z-3, where they interact with a portion of char obtained from CL-1. The gasification products are then directed to cyclone-2 (CL-2) to remove the unconverted char. Later, the solid products are directed to Z-4 while the gaseous products are cooled in the cooler-1 (CR-1). The condensed water from CR-1 is separated in the flash-1 (FL-1) before it is fed to the CO_2-absorber (AS) unit, where the CO_2 is removed from the cooled dry gaseous gasification products. The high-purity CO_2 is directed to Z-4 while other gaseous gasification products are sent to the cooler-2 (CR-2), along with the gas from the cyclone-3 (CL-3). In Z-4, the high-purity CO_2 reacts with a portion of char received from CL-1 and part of gasifying agents (i.e., O_2 and steam). The condensed water from CR-2 is removed in the flash-2 (FL-2) before distributing the syngas to the users. The overall gasification process as described above except the pyrolysis phase majorly contains the following reactions [30]:

Partial oxidation $$C + \frac{1}{2}O_2 \leftrightarrow CO \quad (1)$$

Boudouard reaction $$C + CO_2 \leftrightarrow 2CO \quad (2)$$

Steam reforming $$C + H_2O \leftrightarrow CO + H_2 \quad (3)$$

Water-gas shift reaction $$CO + H_2O \leftrightarrow CO_2 + H_2 \quad (4)$$

Methane reforming $$CH_4 + H_2O \leftrightarrow CO + 3H_2 \quad (5)$$

CO_2 reforming $$CH_4 + CO_2 \leftrightarrow 2CO + 2H_2 \quad (6)$$

Steam reforming of aromatic $$C_xH_yN_z + xH_2O \leftrightarrow xCO + \frac{1}{2}(y + 2x)H_2 + \frac{1}{2}zN_2 \quad (7)$$

p-Cresol steam reforming $$C_7H_8O + 6H_2O \leftrightarrow 7CO + 10H_2 \quad (8)$$

Phenol steam reforming $$C_6H_5OH + 5H_2O \leftrightarrow 6CO + 8H_2 \quad (9)$$

Naphthalene steam reforming $$C_{10}H_8 + 10H_2O \leftrightarrow 10CO + 14H_2 \quad (10)$$

Alkane combustion $$C_nH_{2n+2} + \frac{1}{2}(3n + 1)O_2 \leftrightarrow nCO_2 + (n + 1)H_2O \quad (11)$$

CO combustion $$CO + \frac{1}{2}O_2 \leftrightarrow CO_2 \quad (12)$$

Methane formation $$C + 2H_2 \leftrightarrow CH_4 \quad (13)$$

3. Model development

Performance of the proposed novel gasification process for *Spirulina* is modeled using AspenPlus®, primarily based on the minimization of Gibbs free energy [23,32]. In the simulation, the feedstock *Spirulina* is classified as a nonconventional element while the gasifying agents are categorized as conventional elements. Regarding the solid products, carbon and ash are modeled as cisolid and nonconventional elements, respectively. The gaseous products including H_2, H_2O, CO, CO_2, CH_4, C_2H_6 and tar are considered as conventional elements. It is worth noting that the tar in this simulation is represented by a mixture of indole, benzyl nitrile, benzonitrile, quinolone, p-cresol, phenol and naphthalene. The Peng-Robinson equation of state is chosen as the thermodynamic model due to its good accuracy for simulation of gasification process [23,30,33]. The following assumptions are made: (i) ash is inert; (ii) mass transfer limitation is minimum; and (iii) pressure drop along the equipment is trivial. Operating parameters of the proposed novel gasification process for *Spirulina* are listed in Table 2. The efficiency of the rotating equipment is adapted from the previous literature [19]. In the following, detailed information on the thermodynamic modeling of zones from pyrolysis to optimization is described.

3.1. Pyrolysis zone (Z-1)

Spirulina enters Z-1 with constant mass flow rate of 100 kg/h. In Z-1, the feedstock is thermally decomposed into (a) gaseous products (conventional elements) including H_2, H_2O, CO, CO_2, CH_4, C_2H_6 and tar, (b) carbon (ci-solid element), and (c) ash (nonconventional element). For the thermodynamic modeling of Z-1, the following assumptions are made:

(i) The char only consists of carbon and ash. This has been confirmed through experiment by Fagbemi et al. [34], reporting that a large content of carbon (> 88 wt%) is observed on the char from pyrolysis at 773 K.
(ii) The amount of char is calculated based on the experimental value suggested by Hong et al. [31], showing the char yield from pyrolysis at 973 K.
(iii) The tar is limited to indole, benzyl nitrile, benzonitrile, quinolone, p-cresol, phenol and naphthalene. This is based on the experimental results from Hong et al. [31], where tar was found to be almost composed of nitrogenated compounds, phenols, and polycyclic aromatic hydrocarbons during pyrolysis at 973 K.
(iv) Due to the extreme complexity of the nitrogenated compounds, their thermochemical properties are obtained using the empirical relationship proposed by Benson et al. [35].

The quantity of products as well as heat needed are predicted by

Table 2
Operating conditions of the proposed novel gasification process for *Spirulina* in the simulation.

Inlet temperature of *Spirulina*, boiler feed water and O_2	298 K
Temperature of steam entering gasification zone	623 K
Temperature of pyrolysis zone (Z-1)	973 K
Temperature of combustion zone (Z-2)	1523 K
Temperature of gasification zone (Z-3)	1423 K
Temperature of optimization zone (Z-4)	873 K
Efficiency of BFW pump	0.80
O_2 compressor	
Isentropic efficiency	0.85
Mechanical efficiency	0.96

solving the elemental and heat balances simultaneously in the RYield.

3.2. Combustion zone (Z-2)

The gaseous products obtained from Z-1 then pass CL-1 and contact with the gasifying agents in Z-2, undergoing exothermic reactions which implies to high operating temperature (1523 K). Due to the high temperature in Z-2, reactions in this zone are assumed to reach equilibrium very fast. Therefore, the RGibss block is taken to represent Z-2 in the simulation. RGibss is the only Aspen Plus block which operates according to the minimization of Gibbs free energy method. The products obtained from Z-2 are sent to Z-3 for further processing.

3.3. Gasification zone (Z-3)

In Z-3, the hot gases received from Z-2 react with the solid pyrolysis products from CL-1, resulting in a set of endothermic reactions. Consequently, the temperature of Z-3 is slightly lower than its counterpart in Z-2, as shown in Table 2. However, the temperature in Z-3 is still considered to be adequate to achieve equilibrium. Therefore, the RGibbs block can still be properly used to model Z-3. The products from Z-3 are sent to the gas separation process to remove CO_2 from the syngas stream.

3.4. Optimization zone (Z-4)

The CO_2 from the CO_2-absorber (AS) unit reacts with the unconverted char received from CL-2. In addition, part of char obtained from CL-1 and part of gasifying agents is directed to Z-4. The endothermic reactions in Z-4 lead to the decrease of the operating temperature. Again, an equilibrium condition is assumed to occur at this temperature, where the RGibbs block is employed to model Z-4.

4. Performance evaluation

Performance of a gasification process is usually assessed based on the following aspects: (i) concentration of the targeted syngas products (i.e., primarily H_2 and CO), (ii) cold gas efficiency (CGE), and (iii) gasification system efficiency (GSE). Composition of the syngas is expressed in terms of dry gas basis. The CGE designates the ratio of serviceable energy in the syngas to the reserved energy in the feedstock and steam, which can be expressed as

$$CGE(-) = \frac{m_{sgs} \cdot LHV_{sgs}}{m_{ms} \cdot LHV_{ms} + H_{sm} \cdot m_{sm}}, \quad (14)$$

where m H, and LHV are the mass flow rate, enthalpy and the lower heating value, respectively. The subscript *sgs*, *ms* and *sm* represent the syngas, *Spirulina* and steam, respectively.

GSE accounts for the efficiency of the whole gasification system, which is expressed as

$$GSE = \frac{m_{sgs} \times LHV_{sgs} + Q_{cr-1} + Q_{cr-2}}{m_{ms} \times LHV_{ms} + Q_{z-1} + Q_{z-2} + Q_{z-3} + Q_{z-4} + Q_{br} + E_{c-1} + E_{ox} + E_{as}}, \quad (15)$$

where Q and E are the heat rate and energy rate, respectively. The use of relatively purified O_2 (95% O_2) for gasification is favorable due to its ability to provide a higher gasification temperature which leads to a higher conversion of tar reforming, compared with air [17,30]. Consequently, additional energy of 305 kWh per ton of O_2 is required for the gasification process [36]. An extra energy consumption of 3 MJ/kg of CO_2 absorbed is also involved to run the amine-based CO_2 absorber with the CO_2 removal efficiency of 90% [37].

5. Model validation

The proposed thermodynamic model was first validated by comparing the predicted solid and gaseous pyrolysis products with those of the experimental data reported by Hong et al. [31]. Simulation conditions were set the same as those in the corresponding experiment [31]. The product yields after the pyrolysis stage are summarized Table 3. It can be clearly seen that the proposed thermodynamic model satisfactorily predicts the yield of each product. It is worth noting that the formation of tar is also predicted in this model. As mentioned earlier, tar consists of complex compounds when compared with other specific gaseous products. In addition, the concentration of tar in the syngas is considerably smaller than other species. Therefore, the difference of tar concentration between experiment and this model is reasonable if the above two factors are taken into account.

Table 3
Gas composition of the experimental work [38] and the model.

Compound	Hong et al. [31]	This work	Error (%)
Gaseous product, mol%			
H_2	32.6%	33.4%	2.4%
CO	40.5%	37.8%	6.6%
CH_4	13.8%	15.1%	9.0%
CO_2	7.9%	6.7%	15.4%
C_2H_6	3.0%	3.7%	24.2%
Tar	1.2%	1.5%	24.2%
Solid product, wt%			
Char	10.0%	10.9%	9.4%

6. Results and discussion

The proposed novel gasification configuration is first evaluated by the foregoing developed thermodynamic model, at a constant feedstock feed rate of 100 kg/h. The temperatures of the pyrolysis zone (Z-1), combustion zone (Z-2), gasification zone (Z-3), and optimization zone (Z-4) are maintained constant at 973 K, 1523 K, 1423 K and 873 K, respectively. Then, the effects of O_2 equivalence ratio and steam injection on process performance are investigated.

6.1. Process description

As mentioned above, the overall gasification process consists of four primary steps, in which the pyrolysis step converts the *Spirulina* feedstock into char and pyrolysis gas products, the combustion step reforms tar into the desired permanent gases, the gasification step converts char into syngas and the optimization step transforms unconverted char into valuable gases with the help of the recycled CO_2. Pure oxygen and steam are fed into the system with an oxygen equivalence ratio (O_2 ER ratio) of 0.3 and steam to carbon (S/C) ratio of 1.0. The O_2 ER ratio defined as the ratio of actual oxygen to biomass ratio to the stoichiometric oxygen to biomass ratio. The S/C ratio is the molar ratio of steam to carbon in the biomass. Before entering the gasifier, the steam flow is split into two streams. One stream, containing 80% of the fed steam, enters the combustion zone (Z-2) and the other stream (20%) goes to the optimization zone (Z-4). On the other hand, oxygen is directly introduced to the combustion zone (Z-2). The char from the cyclone-1 (CL-1) is split into two streams and sent to gasification zone (Z-3) and optimization zone (Z-4). In this regard, the optimization zone (Z-4) is selected as a reference for quantifying the char split in term of mass fraction, called C to Z-4. Thus, when the entire char stream is directed to the gasification zone (Z-3), the condition is referred as C to Z-4 of 0.0.

Fig. 2 shows the molar flow rates of the major constituents of the feed and the products streams of each primary zone. It is clearly seen in Fig. 2a that the product streams contains tar, carbon and light gases including H_2, CO, CO_2, CH_4, C_2H_6, O_2, N_2 and H_2O. This result indicates that in the pyrolysis stage, the *Spirulina* biomass is completely decomposed into gaseous products and tar. The low temperature of the pyrolysis stage (973 K) favors the conversion of *Spirulina* biomass into tar

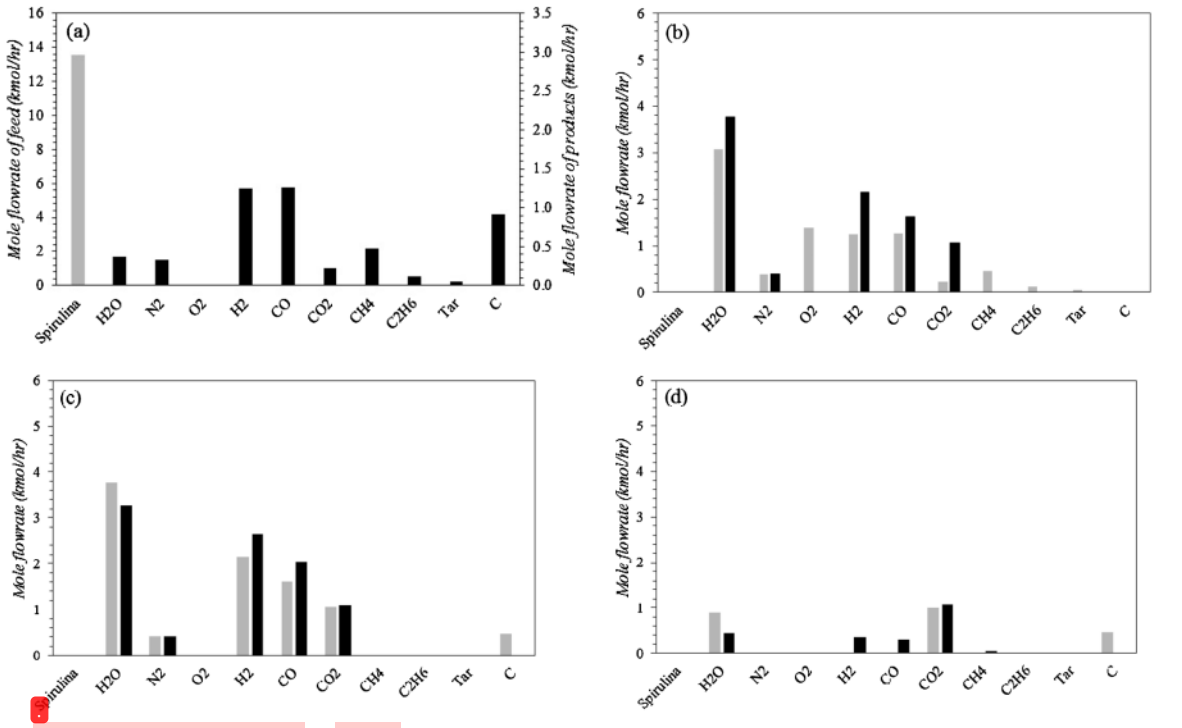

Fig. 2. Mole flow of the feed and product of (a) pyrolysis zone, (b) combustion zone, (c) gasification zone, and (d) optimization zone. (Feed: grey; product: black).

[38–40]. Following the pyrolysis step, the mixed product stream is sent to cyclone-1 (CL-1) in order to separate solids from the rest of the products. The separated solid products is sent to the splitter for splitting the char to: (1) the gasification zone (Z-3) and (2) the optimization zone (Z-4), while the gaseous products including tar are sent to the combustion zone (Z-2) for further processing.

In the combustion zone (Z-2), the gaseous pyrolysis products react with the gasifying agents (O_2 and steam) to permanent gases. As a result, the molar flow rates of CH_4, C_2H_6 and O_2 in the product stream significantly decrease, while the flow rates of H_2O and CO_2 increase (Fig. 2b). The exothermic alkane combustion reactions also increase the combustion zone temperature up to 1523 K. This high temperature facilitates the tar reforming reactions (Eqs. (7)–(10)) and converts tar into the permanent gases. This is confirmed by the absence of tar in the product stream. The tar reforming reactions also contribute to the production of H_2 and CO [30]. The combustion zone (Z-2) products flows to the gasification zone (Z-3) for further reactions.

In gasification zone (Z-3), the combustion products react with char received from the cyclone-1 (CL-1). Consequently, the carbon feed rates of the product stream decreases, while the reform products (H_2 and CO) increase, as shown in Fig. 2c. This observation indicates that the steam reforming reaction (Eq. (3)) dominates in the gasification stage. The flow rate of CO_2 in the product stream is slightly higher than its counterpart in the feed stream. This suggests the participation of the water-gas shift reaction (Eq. (4)), which is also confirmed by the decrease flow rate of H_2O. The gasification products from Z-3 is sent to the gas treatment process including Cyclone-2 (CL-2) and CO_2-absorber (AS) to remove the unconverted char and CO_2 from the main syngas stream, respectively.

In the optimization zone (Z-4), char received from the cyclone-2 (CL-2) and cyclone-1 (CL-1), reacts with pure CO_2 and steam, received from the CO_2-absorber (AS) and the boiler (BR), respectively. In Z-4, char reacts with the oxidizing agents converting C and CO_2 into CO (Eqs. (2) and (4)). This is confirmed by disappearance of carbon and increase of CO flow rates in the product stream (Fig. 2d). Interesting to see (in Fig. 2d) that the overall CO_2 flow slightly increases, despite its consumption in reaction Eq. (2). This increase of CO_2 can be explained by comparing CO_2 and H_2 production via water-gas shift reaction (Eq. (4)), which results in a higher flow rate of H_2. The slight increase of H_2 flow rate is due to hydrogen consumption in methanation reaction (Eq. (13)) to give CH_4.

6.2. The effects of O_2 equivalence ratio

The effect of O_2 equivalence ratio (ER) (varied from 0.00 to 1.00) on the gasification performance is investigated at a constant S/C ratio of 1.0. The char supplied to Z-4 is varied between 0 and 0.6 (as a fraction of total char flow) to study the effect of char split configuration at various O_2 split fractions (O_2 to Z-4 is varied between 0.0 and 0.4).

The dry basis concentrations of the primary constituents (H_2, CO and CO_2) in the syngas at various splits of char and oxygen for the O_2 ER from 0.00 to 1.00 are shown in Fig. 3. It can be clearly seen that increasing O_2 ER at a certain value favors CO_2 production and decreases the concentrations of H_2 and CO. Further increase in O_2 ER after the optimal point has minimum influence on the syngas composition. Indeed, the production of CO and H_2 is dominated by partial oxidation reaction (Eq. (1)) and steam reforming reaction (Eq. (3)). However, the presence of excessive O_2 in the gasification system promotes CO oxidation reaction (Eq. (12)), resulting in CO_2 formation and restrain the concentrations of CO and H_2. The reason for the plateau (Figs. 3a and 4a) of syngas composition at high O_2 ER can be explained by the absence of CO due to the lack of carbon source from char. The CO concentration is near to zero, where a complete carbon conversion is reached at very high O_2 ER (O_2 ER $>$ 0.92 when the C to Z-4 equals 0). Similar result is observed on the other char split fractions. These results indicate that higher amount of O_2 in the gasification process is responsible for the CO oxidation to CO_2 (Eq. (12)), leading to minimum CO production. Billdaud et al. [41] also reported similar conclusion

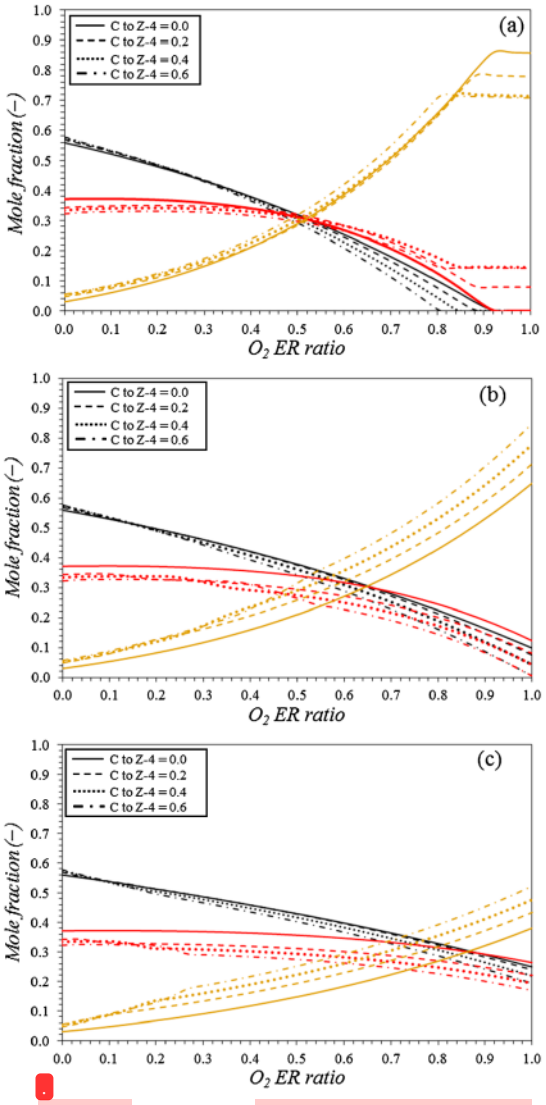

Fig. 3. The effect of O_2 equivalence ratio on the composition of syngas at different O_2 to Z-4 fractions: (a) O_2 to Z-4 of 0.0, (b) O_2 to Z-4 of 0.2 and (c) O_2 to Z-4 of 0.4. (Red: CO, black: H_2 and brown: CO_2). (For interpretation of the references to colour in this figure legend, the reader is referred to the web version of this article.)

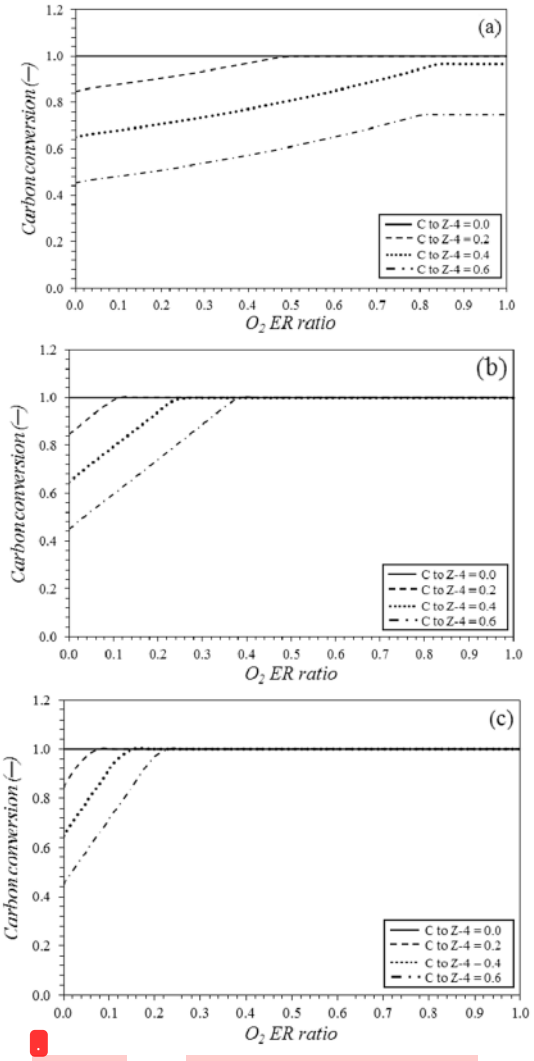

Fig. 4. The effect of O_2 ER ratio on carbon conversion at different O_2 to Z-4 fractions: (a) O_2 to Z-4 of 0.0, (b) O_2 to Z-4 of 0.2 and (c) O_2 to Z-4 of 0.4.

with a set of gasification experiments using beech wood as the feedstock. In their experiments, the highest CO concentration (24 mol/kg feedstock) was observed when O_2 ER is around 0.42. CO concentration decreased from 24 to 11 mol/kg feedstock with the increase of O_2 ER from 0.42 to 0.60.

The variation of char fed (as fraction) to Z-4 has a significant impact on the syngas composition (Fig. 4a). At high char flow and low O_2 ER, the concentrations of CO_2 and H_2 slightly increase while the concentration of CO decreases. However, the influence of char on the syngas composition fades as the O_2 ER is elevated up to a certain value. When the O_2 ER exceeds this threshold, the effect of char split becomes more prominent. The reason for this behavior comes from the fact that at this configuration O_2 is primarily sent to Z-2, which contributes to the combustion and provides high temperature and high steam H_2O concentration that facilitate the char conversion through the steam reforming reaction (Eq. (3)). At minimum char flow to the optimization zone (Z-4), the char is mainly fed to the gasification zone (Z-3), and converted into CO. It is worth noting that higher char fraction to optimization zone (Z-4) has a positive influence on CO concentration, while a negative effect is found on CO_2 concentration, especially at high O_2 ER ratio. The reason of this lays on the fact that the increase of char split to the optimization zone (Z-4) retards carbon conversion, which leads to low activity of CO combustion reaction (Eq. (12)) due to the limited CO concentration.

As mentioned above, O_2 is split into the combustion zone (Z-2) and the optimization zone (Z-4). The split fraction of O_2 to the optimization zone (Z-4) has a considerable influence on the syngas composition, by comparing Fig. 3a–c. The increase of O_2 split fraction to optimization zone (Z-4) minimizes the effect of O_2 ER ratio on the syngas composition. For example, as it can be seen in Fig. 3a that the concentration of H_2 drastically decreases from 0.58 to 0.29 with increase of O_2 ER ratio from 0.0 to 0.5 at the C to Z-4 and the O_2 to Z-4 of 0.6 and 0.0. Under similar situation, a slower reduction rate of H_2 concentration

(0.58–0.40) is observed when the O_2 to Z-4 is elevates from 0.0 to 0.4. This result indicates that the formation of syngas constituents primarily determines in the combustion zone (Z-2) and gasification zone (Z-3) due to its opportunity to receive a rich mixture of products from the pyrolysis stage (Z-1). Consequently, the presence of O_2 at higher level in the combustion zone (Z-2) has stronger control to the syngas composition given it affects the product of the gasification zone (Z-3) when compared to its counterpart in the optimization zone (Z-4), which handles a smaller number of feed compounds (mainly only char and CO_2). The identical fashion is found on the concentration of CO and CO_2.

In line with the syngas composition, the split fraction of O_2 to optimization zone (Z-4) also has a strong effect on the carbon conversions (Fig. 4). The addition of O_2 to the optimization zone (Z-4) with the O_2 to Z-4 of 0.4 slightly reduces the O_2 requirement (O_2 ER ratio of 0.08) to achieve a complete carbon conversion. This result can be explained by the fewer number of species that is involved in the optimization zone (Z-4) as compared to the species in the gasification zone (Z-2). Therefore, in the optimization zone (Z-4) the O_2 supply is exclusively reacted with char through the partial oxidation reaction (Eq. (1)). In addition, the presence of pure CO_2 from the CO_2-absorber (AS) facilitates char conversion by Bouduard reaction (Eq. (2)).

The significant influence of O_2 is also observed on the CGE, as shown in Fig. 5. It can be clearly seen in Fig. 5a that the CGE continuously decreases with the increase of O_2 ER ratio up to a certain condition in the gasification with the O_2 to Z-4 of 0.0. Further increase of O_2 supply above that O_2 ER ratio value has a negligible influence on the CGE. This result indicates that the CGE is strongly influenced by the syngas composition. The lower concentration of combustible species in the syngas due to the increase of O_2 ER ratio leads to a lower CGE. In addition, the sustained CGE with the increase of O_2 ER ratio can be related to the constant syngas composition at high O_2 ER ratio. This is confirmed by the CGE with the O_2 to Z-4 of 0.2 and 0.4 as depicted in Fig. 5b and c, respectively. Similar conclusion is previous drawn by Adnan et al. [19], reporting an adverse influence of the increase of O_2 injection to the gasification of various feedstock on the CGE.

The O_2 also has a considerable effect on the GSE, as depicted in Fig. 5. One can see in Fig. 5a that the increase of O_2 ER ratio has an adverse effect on the GSE to the minimum GSE value. Further increase of O_2 ER ratio has a negligible influence on the GSE. Again, this finding indicates that the syngas composition has a strong influence on the GSE. The similar conclusion is reported in the previous studies [19,30].

6.3. The effects of steam injection

The parametric study on the effect of steam is carried out by introducing a various boiler feed water with the S/C ratio of 0.0–2.0 at a constant *Spirulina* flow rate of 100 kg/h. In this S/C ratio parametric study, O_2 is added to the combustion zone (Z-2) at O_2 ER ratio of 0.25. The char split fraction to the optimization zone (Z-4) is varied between the C to Z-4 of 0.0 to 0.6 in order to study the effect of char at various steam split fractions to the optimization zone (Z-4) with the steam to Z-4 from 0.0 to 0.4.

Fig. 6 plots the effect of S/C ratio on dry basis syngas composition at various char and steam split fraction into the optimization zone (Z-4). It can be clearly seen from this figure that the S/C ratio significantly affects the syngas composition. The addition, steam has a positive influence on the concentration of H_2 and CO_2, while an adverse effect is found on CO concentration. This can be explained by the fact that the increase of H_2O amount in the gasification process facilitates water-gas shift reaction (Eq. (4)), consuming CO and H_2O to produce CO_2 and H_2. As per CO species, it is worth noting that the CO as a reactant of water-gas shift reaction (Eq. (4)) is produced from the conversion of carbon with the steam through reforming reaction (Eq. (3)). This is confirmed by the increase of carbon conversion with increasing S/C ratio as depicted in Fig. 7a. The present result found a good agreement with the

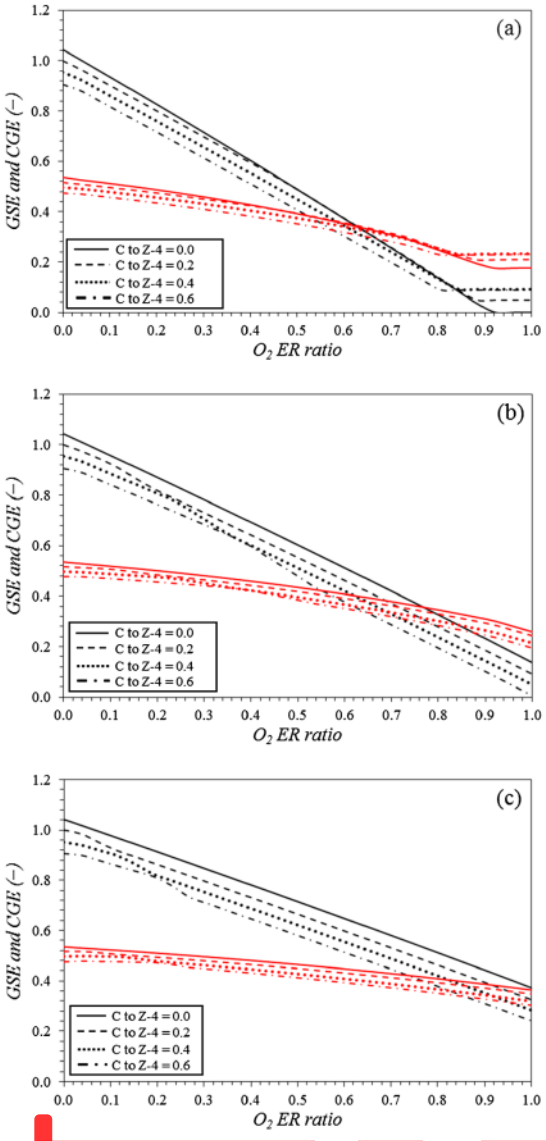

Fig. 5. The effect of equivalence ratio on GSE (red) and CGE (black) at different O_2 to Z-4 fractions: (a) O_2 to Z-4 of 0.0, (b) O_2 to Z-4 of 0.2 and (c) O_2 to Z-4 of 0.4. (For interpretation of the references to colour in this figure legend, the reader is referred to the web version of this article.)

previous experimental investigation by Li et al. [42] on the gasification using a corn stalk as the feedstock. In addition, steam contributes a considerable amount of hydrogen source for reforming reaction [43]. Similar trend is also found in the gasification with the steam to Z-4 of 0.2 and 0.4 with slight different values, as depicted in Fig. 6b and c, respectively. The char split ratio to the optimization zone (Z-4) has a minimum influence of the syngas composition. At the low S/C ratio, the concentration of CO and H_2 diminish while the CO_2 concentration elevates when the C to Z-4 is increased from 0.0 to 0.6. At high S/C ratio the opposite trend is found on the CO concentration. For instance, the CO_2 concentration slightly augments from 0.04 to 0.07 while the concentration of CO and H_2 slightly decreases from 0.41 to 0.40 and 0.49 to 0.46, respectively, when the C to Z-4 was increased from 0.0 to

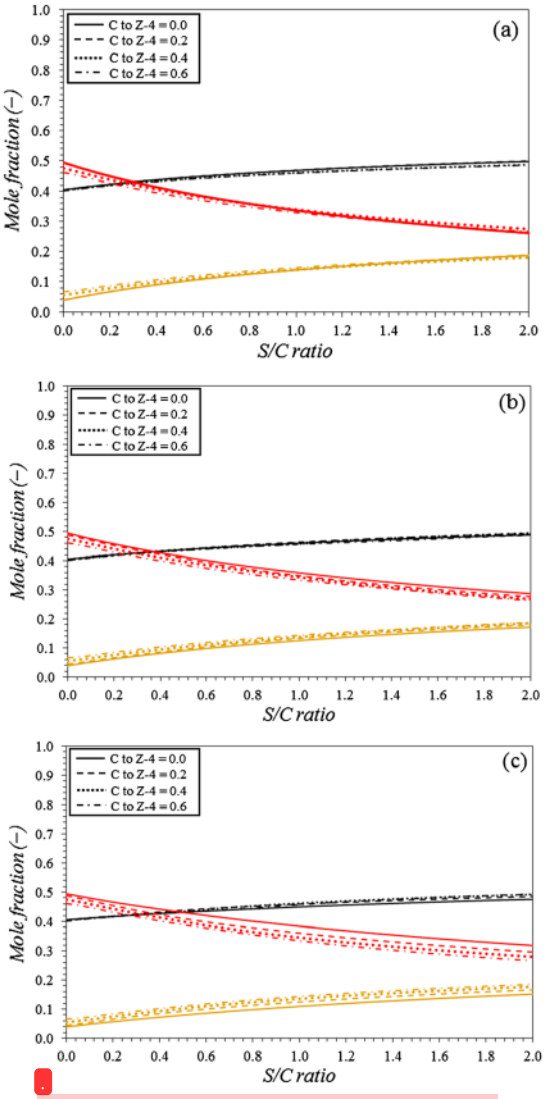

Fig. 6. The effect of S/C ratio on the composition of syngas at different steam to Z-4 fractions: (a) steam to Z-4 of 0.0, (b) steam to Z-4 of 0.2 and (c) steam to Z-4 of 0.4. (Red: CO, black: H_2 and brown: CO_2). (For interpretation of the references to colour in this figure legend, the reader is referred to the web version of this article.)

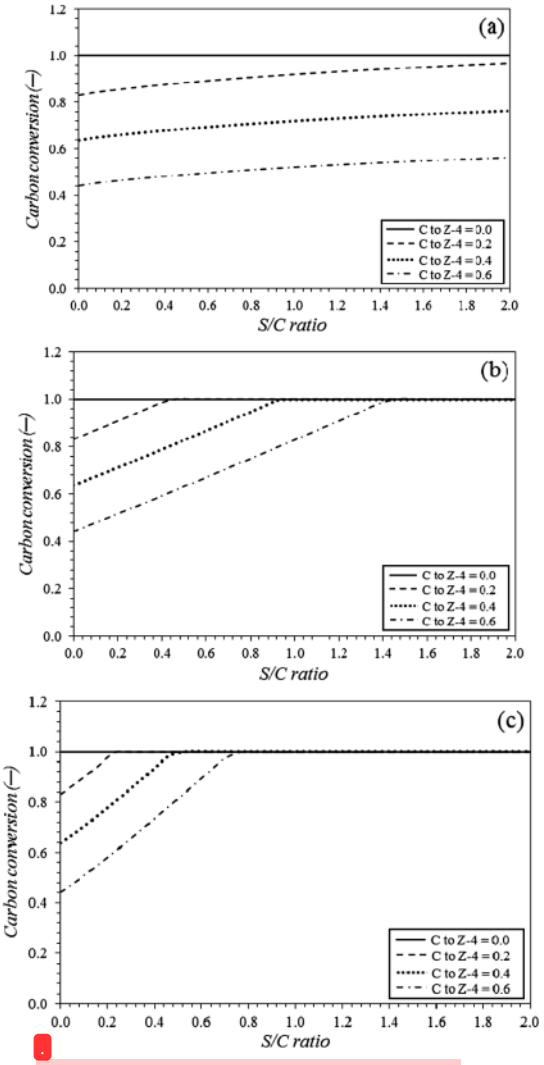

Fig. 7. The effect of S/C ratio on carbon conversion at different steam to Z-4 fractions: (a) steam to Z-4 of 0.0, (b) steam to Z-4 of 0.2 and (c) steam to Z-4 of 0.4.

0.6 on the gasification with the steam to Z-4 and the S/C ratio of 0.0 and 0.31, respectively. Under the similar conditions with higher S/C ratio (2.00), the concentration of CO slightly raises from 0.26 to 0.27 while the concentration of H_2 declined from 0.50 to 0.49 and the CO_2 concentration remains constant at 0.19. The explanation of this lays on the fact that the steam reforming reaction (Eq. (3)) has a minor influence on the syngas composition due to the small amount of char from the pyrolysis product (i.e., 10 wt%). The limited CO concentration leads to the minimum effect of the water-gas shift reaction (Eq. (4)). This is confirmed by the significant increase of carbon conversion that is not in line with the increase of CO concentration in the syngas as depicted in Figs. 7 and 6, respectively.

The influence of the char split fraction the optimization zone (Z-4) on the syngas concentration is higher when the steam split fraction to the optimization zone (Z-4) is increased from 0.0 to 0.4, as shown in Fig. 6a–c. This can be explained by the fact that the steam reforming reaction (Eq. (3)), which is promoted by steam injection, facilitates conversion of carbon and steam into CO and H_2. It is worth noting that at higher steam to Z-4, the domination of the water-gas shift (Eq. (4)) reaction increases due to the excess amount of steam, converting CO and steam into CO_2 and H_2.

The considerable effect of steam at various char split fraction to the optimization zone (Z-4) is also found on the CGE, as depicted in Fig. 8. The CGE slightly mitigates with the increase of S/C ratio from 0.0 to 2.0 at the C to Z-4 of 0.0. These results can be explained by the fact that the increase of heating value due to the slight increase of H_2 concentration is counterbalanced by the significant decrease of CO concentration, resulting a decline of net syngas heating value. This is an indication of strong influence of syngas composition on the CGE. The similar fashion is observed on the gasification with the steam to Z-4 of 0.2 and 0.4, as shown in Fig. 8b and c, respectively. The identical conclusion is reported in the previous published literature [19]. The char split fraction to the optimization zone (Z-4) has a negative effect on the CGE at low

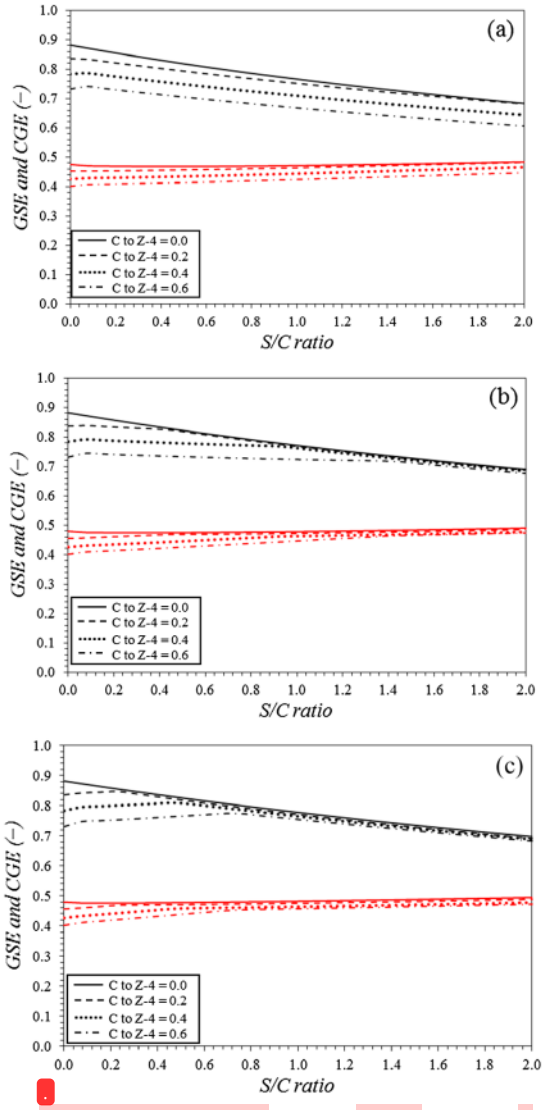

Fig. 8. The effect of S/C ratio on GSE (red lines) and CGE (blak lines) at different steam to Z-4 fractions: (a) steam to Z-4 of 0.0, (b) steam to Z-4 of 0.2 and (c) steam to Z-4 of 0.4.

S/C ratio. The influence of the char split fraction diminishes at higher S/C ratios. This indicates that lower carbon conversion results in lower CGE due to the reduction of syngas flow rate. This is confirmed by the decrease of carbon conversion at higher C to Z-4, as depicted in Fig. 7.

The steam also has a positive influence on the GSE, as shown in Fig. 7. One can see from this figure that the GSE slightly increases from 0.47 to 0.48 with the increase of S/C ratio from 0.0 to 2.0 for the gasification with C to Z-4 and C to Z-4 of 0.0 and 0.0, respectively (Fig. 7a). The higher increase of GSE is observed on higher char split fraction to the optimization zone (Z-4). For instance, on the gasification at the C to Z-4 of 0.6, the GSE significantly elevates from 0.40 to 0.45 with the increase of S/C ratio from 0.0 to 2.0 for steam to Z-4 of 0.0. The identical fashion is observed on the steam to Z-4 of 0.2 and 0.4 as depicted in Fig. 7b and c, respectively. This indicates that the addition of steam facilitates an exothermic CO combustion reaction (12) given the steam promotes steam reforming reactions (Eq. (3)) which produce CO. This is confirmed by the increase of CO_2 concentration as the S/C ratio is elevated, as depicted in Fig. 6.

7. Conclusions

A new biomass gasification configuration is developed using Aspen Plus software, considering the formation of tar during the pyrolysis stage. The *Spirulina* microalgae is considered as the biomass feedstock. Following are the conclusion of this study:

i. The performances (syngas composition, cold gas efficiency and gasification system efficiency) of gasification process vary with different char, O_2 and steam split fraction to the optimization zone (Z-4).
ii. The use of suitable amount of oxygen (O_2 ER) as a gasifying agent enables a complete reforming of tar into syngas in the combustion zone (Z-2).
iii. The use of steam as a gasifying agent facilitates H_2 production. The highest H_2 concentration (0.58) is observed on the gasification at O_2 ER ratio and S/C ratio of 0.0 and 1.0, respectively, for char to Z-4 and O_2 to Z-4 of 0.6 and 0.0, respectively.
iv. The highest CGE (1.04) and GSE (0.52) is found in gasification at the O_2 ER ratio, the S/C ratio and C to Z-4 of 0.0, 1.0, 0.0, respectively for all studied O_2 to Z-4 (0.0, 0.2, and 0.4).
v. The inclusion of the optimization zone (Z-4) promotes the concentration of CO and H_2 at the controlled use of gasifying agents.

Acknowledgements

The author(s) would like to acknowledge the financial support provided by the Deanship of Scientific Research (DSR) at King Fahd University of Petroleum & Minerals (KFUPM) for funding this work through project No. IN161022. We also would like to acknowledge the supports from the directorate of research and community services at Islamic University of Indonesia (DPPM-UII).

References

[1] de Lasa H, Salaices E, Mazumder J, Lucky R. Catalytic steam gasification of biomass: catalysts, thermodynamics and kinetics. Chem Rev 2011;111:5404.
[2] Nautiyal P, Subramanian KA, Dastidar MG. Production and characterization of biodiesel from algae. Fuel Process Technol 2014;120:79.
[3] Adnan MA, Hossain MM. CO_2 gasification of microalgae (N. Oculata) – a thermodynamic study. MATEC Web Conf 2018;154:01002.
[4] Adnan MA, Hossain MM. Co-gasification of Indonesian coal and microalgae – a thermodynamic study and performance evaluation. Chem Eng Process - Process Intensif 2018;128:1.
[5] Slade R, Bauen A. Micro-algae cultivation for biofuels: cost, energy balance, environmental impacts and future prospects. Biomass Bioenergy 2013;53:29.
[6] Park H, Lee C-G. Theoretical calculations on the feasibility of microalgal biofuels: utilization of marine resources could help realizing the potential of microalgae. Biotechnol J 2016;11:1461.
[7] Richardson JW, Johnson MD, Lacey R, Oyler J, Capareda S. Harvesting and extraction technology contributions to algae biofuels economic viability. Algal Res 2014;5:70.
[8] Valderrama Rios ML, González AM, Lora EES, Almazán del Olmo OA. Reduction of tar generated during biomass gasification: a review. Biomass Bioenergy 2018;108:345.
[9] Jia S, Ning S, Ying H, Sun Y, Xu W, Yin H. High quality syngas production from catalytic gasification of woodchip char. Energy Convers Manage 2017;151:457.
[10] Anis S, Zainal ZA. Tar reduction in biomass producer gas via mechanical, catalytic and thermal methods: a review. Renew Sust Energ Rev 2011;15:2355.
[11] Guan G, Kaewpanha M, Hao X, Abudula A. Catalytic steam reforming of biomass tar: Prospects and challenges. Renew Sust Energy Rev 2016;58:450.
[12] Fagbemi L, Khezami L, Capart R. Pyrolysis products from different biomasses: application to the thermal cracking of tar. Appl Energy 2001;69:293.
[13] Jiang L, Liu C, Hu S, Wang Y, Xu K, Su S, et al. Catalytic behaviors of alkali metal salt involved in homogeneous volatile and heterogeneous char reforming in steam gasification of cellulose. Energy Convers Manage 2018;158:147.
[14] Abu El-Rub Z, Bramer EA, Brem G. Review of catalysts for tar elimination in biomass gasification processes. Ind Eng Chem Res 2004;43:6911.
[15] Mazumder J, De Lasa H. Fluidizable Ni/La2O3-γAl2O3 catalyst for steam gasification of a cellulosic biomass surrogate. Appl Catal B 2014;160–161:67.
[16] Adnan MA, Muraza O, Razzak SA, Hossain MM, de Lasa HI. Iron oxide over silica-

doped alumina catalyst for catalytic steam reforming of toluene as a surrogate tar biomass species. Energy Fuels 2017;31(7):7471–81.
[17] Susanto H, Beenackers AACM. A moving-bed gasifier with internal recycle of pyrolysis gas. Fuel 1996;75:1339.
[18] Brandt P, Larsen E, Henriksen U. High tar reduction in a two-stage gasifier. Energy Fuels 2000;14:816.
[19] Adnan MA, Hossain MM. Gasification performance of various microalgae biomass – a thermodynamic study by considering tar formation using Aspen plus. Energy Convers Manage 2018;165:783.
[20] Tang Y, Liu J. Effect of anode and Boudouard reaction catalysts on the performance of direct carbon solid oxide fuel cells. Int J Hydrogen Energy 2010;35:11188.
[21] Masmoudi MA, Halouani K, Sahraoui M. Comprehensive experimental investigation and numerical modeling of the combined partial oxidation-gasification zone in a pilot downdraft air-blown gasifier. Energy Convers Manage 2017;144:34.
[22] Adnan MA, Hossain MM. Gasification of various biomasses including microalgae using CO_2 – a thermodynamic study. Renew Energy 2018;119:598.
[23] Adnan MA, Susanto H, Binous H, Muraza O, Hossain MM. Feed compositions and gasification potential of several biomasses including a microalgae: a thermodynamic modeling approach. Int J Hydrogen Energy 2017;42:17009.
[24] Fortunato B, Brunetti G, Camporeale SM, Torresi M, Fornarelli F. Thermodynamic model of a downdraft gasifier. Energy Convers Manage 2017;140:281.
[25] Han J, Liang Y, Hu J, Qin L, Street J, Lu Y, et al. Modeling downdraft biomass gasification process by restricting chemical reaction equilibrium with Aspen Plus. Energy Convers Manage 2017;153:641.
[26] Xiang X, Gong G, Shi Y, Cai Y, Wang C. Thermodynamic modeling and analysis of a serial composite process for biomass and coal co-gasification. Renew Sust Energ Rev 2018;82:2768.
[27] Zhang X, Li H, Liu L, Bai C, Wang S, Zeng J, et al. Thermodynamic and economic analysis of biomass partial gasification process. Appl Therm Eng 2018;129:410.
[28] Gopaul SG, Dutta A, Clemmer R. Chemical looping gasification for hydrogen production: a comparison of two unique processes simulated using ASPEN Plus. Int J Hydrogen Energy 2014;39:5804.
[29] Mostafavi E, Pauls JH, Lim CJ, Mahinpey N. Simulation of high-temperature steam-only gasification of woody biomass with dry-sorption CO_2 capture. Can J Chem Eng 2016;94:1648.
[30] Adnan MA, Susanto H, Binous H, Muraza O, Hossain MM. Enhancement of hydrogen production in a modified moving bed downdraft gasifier – a thermodynamic study by including tar. Int J Hydrogen Energy 2017;42:10971.
[31] Hong Y, Chen W, Luo X, Pang C, Lester E, Wu T. Microwave-enhanced pyrolysis of macroalgae and microalgae for syngas production. Bioresour Technol 2017;237:47.
[32] Renganathan T, Yadav MV, Pushpavanam S, Voolapalli RK, Cho YS. CO_2 utilization for gasification of carbonaceous feedstocks: a thermodynamic analysis. Chem Eng Sci 2012;83:159.
[33] Yan L, He B. On a clean power generation system with the co-gasification of biomass and coal in a quadruple fluidized bed gasifier. Bioresour Technol 2017;235:113.
[34] Fagbemi L, Khezami L, Capart R. Pyrolysis products from different biomasses. Appl Energy 2001;69:293.
[35] Benson SW, Cruickshank FR, Golden DM, Haugen GR, O'Neal HE, Rodgers AS, et al. Additivity rules for the estimation of thermochemical properties. Chem Rev 1969;69:279.
[36] Tijmensen MJA, Faaij APC, Hamelinck CN, van Hardeveld MRM. Exploration of the possibilities for production of Fischer Tropsch liquids and power via biomass gasification. Biomass Bioenergy 2002;23:129.
[37] Peters L, Hussain A, Follmann M, Melin T, Hägg MB. CO2 removal from natural gas by employing amine absorption and membrane technology—a technical and economical analysis. Chem Eng J 2011;172:952.
[38] Duman G, Uddin MA, Yanik J. Hydrogen production from algal biomass via steam gasification. Bioresour Technol 2014;166:24.
[39] Stark AK, Bates RB, Zhao Z, Ghoniem AF. Prediction and validation of major gas and tar species from a reactor network model of air-blown fluidized bed biomass gasification. Energy Fuels 2015;29:2437.
[40] Stark AK, Ghoniem AF. Quantification of the influence of particle diameter on Polycyclic Aromatic Hydrocarbon (PAH) formation in fluidized bed biomass pyrolysis. Fuel 2017;206:276.
[41] Billaud J, Valin S, Peyrot M, Salvador S. Influence of H_2O, CO_2 and O_2 addition on biomass gasification in entrained flow reactor conditions: experiments and modelling. Fuel 2016;166:166.
[42] Li B, Yang H, Wei L, Shao J, Wang X, Chen H. Hydrogen production from agricultural biomass wastes gasification in a fluidized bed with calcium oxide enhancing. Int J Hydrogen Energy 2017;42:4832.
[43] Shayan E, Zare V, Mirzaee I. Hydrogen production from biomass gasification; a theoretical comparison of using different gasification agents. Energy Convers Manage 2018;159:30.

Gasification performance of Spirulina microalgae_A thermodynamic study with tar formation

ORIGINALITY REPORT

8%	8%	0%	0%
SIMILARITY INDEX	INTERNET SOURCES	PUBLICATIONS	STUDENT PAPERS

MATCH ALL SOURCES (ONLY SELECTED SOURCE PRINTED)

6%

★ uspto.report

Internet Source

Exclude quotes	On	Exclude matches	< 2%
Exclude bibliography	On		